

Thermodynamic and dynamic anomalous behavior in the TIP4P/ ε water model

Raúl Fuentes-Azcatl and Marcia C. Barbosa

*Instituto de Física, Universidade Federal do Rio Grande do Sul,
Caixa Postal 15051, 91501-970, Porto Alegre, RS, Brazil*

E-mail:

*To whom correspondence should be addressed

Abstract

The model Tip4p/ ϵ for water is tested for the presence of thermodynamic and dynamic anomalies. Molecular dynamic simulations for this model were performed and we show that for this system the density versus temperature at constant pressure exhibits a maximum. In addition we also show that the diffusion coefficient versus density at constant temperature has a maximum and a minimum. The anomalous behavior of the density and of the diffusion coefficient obey the water hierarchy. The results for the Tip4p- ϵ are consistent with experiments and when compared with the Tip4p-2005 model show similar results a variety of physical properties and better performance for the dielectric constant.

Introduction

Water is a fascinating molecule. Even though present in our everyday life, it shows a number of properties that are still not well described.^{1,2} For example, most liquids contract upon cooling. This is not the case of water, a liquid where the specific volume at ambient pressure starts to increase when cooled below 4°C at atmospheric pressure.³ In addition, in a certain range of pressures, water also exhibits an anomalous increase of compressibility and of the specific heat upon cooling.^{4–6} Water also has dynamic anomalies. Experiments show that the diffusion constant, D , increases on compression at low temperature, T , up to a maximum $D_{\max}(T)$ at $p = p_{D\max}(T)$. The behavior of normal liquids, with D decreasing on compression, is restored in water only at high p , e.g. for $p > p_{D\max} \approx 1.1$ kbar at 10°C.⁷

In addition to the measured anomalies of water, theoretical analysis predicted anomalies^{2,8} that are located in regions of the pressure versus temperature phase diagram of difficult access experimentally. Consequently, simulations became an interesting tool to test these theories. Then the challenge faced when developing a computational strategy is to design a model that would be general enough to describe the different behaviors of water and simple enough to be computationally treatable. The later prerequisite at the moment preclude the

consideration of quantum effects and polarization. Both polarization and quantum effects, however, seems to play a relevant role in the anomalous properties of water particularly when charges and interfaces are present. In order to circumvent this difficulty without loosing the simplicity required for simulation purposes, a number of atomistic models has been developed with the assumption that polarization and quantum effects were included in an averaged way.

These atomistic models are characterized by representing the charges in water by two, three, four or even five points. Then, the interactions were modelled by a classical Lennard-Jones for the hardcore interactions and the electrostatic interactions for the charges. This leads to the following parameters that need to be specified: the values and positions of the charges, the positions and masses of the atoms and the energy and size for the LJ interaction. Then, the crucial step in the modelling process is the choice of the set of quantities used to fit these parameters. This set should be small but appropriated to guarantee that the model reproduces as many properties of water as possible at least in a certain range of temperatures and pressures.

Within the non-polarizable models the 4-site form represented an advance. It was first proposed by Bernal and Fowler⁹ along with a set of parameters based on calculations for properties of the monomer, dimer, and ice. The fours points are the position of the oxygen and hydrogens and the location , M , of the negative charge. Within the Tip4p each hydrogen carries a positive charge, q_H , while the negative charge, q_M is located at a position r_{OM} from the oxygen between the two hydrogens. The angle between the oxygens and the hydrogens, 104.52° , and the distance between the oxygen and the hydrogen, $r_{OH} = 0.9572$, where fixed to reproduce the ice structure. The Bernal and Fowler model, however, gives a poor results for the liquid properties at room $25^\circ C$ and atmospheric pressure. A reparametrization of this model gave rise to the TIP4P¹⁰ model that shows good agreement with the density at $25^\circ C$ and 1 atm and an excellent value for the vaporization enthalpy. In addition this model provides a reasonable description of some solid phases and reproduces qualitatively

the phase diagram^{11–14} while the results for the SPC/E and TIP5P models are quite poor. Unfortunately it gives a value that is too low for the temperature of maximum density and of melting. Then, it became clear that good model of water should provide the behavior of the liquid, particularly the value of the density anomaly at atmospheric pressure, and a reasonable description of the solid phases. For that purpose the TIP4P/2005¹² was created. It was designed to match the density at the temperature of maximum density but yields a slightly low melting temperature and a somewhat large vaporization enthalpy.

In order to test the TIP4P/2005 model against other options, Vega et al.¹⁴ have compared a number of the non-polarizable models. The strategy was to select a set of water properties and compared the results obtained by different models with the experiments. They established that the best model to reproduce the properties they have selected is the four sites TIP4P/2005^{12,13} followed by the three sites SPC/E model.¹⁵ The only drawback of these models is that they do not give a good description for the dielectric constant of water. Since the dielectric constant is fundamental for understanding the behavior of mixtures of water and other substances, particularly polar molecules, these water models are not appropriated to analyse these mixtures.

In order to circumvent this difficulty without loosing the advantages of the TIP4P/2005,^{12,13} Fuentes et al.¹⁷ developed the non-polarizable TIP4P/ ϵ rigid model. This potential is parametrized to give the experimental value of the density and of the dielectric constant at 4°C and atmospheric pressure. This new model showed that it is capable of reproducing some thermodynamic quantities¹⁷ obtained by the TIP4P/2005.^{12,13} In addition it gives a good agreement with the experiments for the isothermal compressibility and dielectric constant at different pressures and temperatures what is not observed in the non-polarizable models.

In addition to the thermodynamic anomalies, water also show a singular mobility. While experimental results show that the diffusion coefficient of water decreases with decreasing pressures up to crystallization, simulations with SPC/E water show that this system if kept

liquid reaches a minimum^{18–20} at negative pressures. Then the pressure and the temperature of the maximum and the minimum of the mobility define a region of diffusion anomaly. This region englobes the density anomaly defining the hierarchy of the anomalies.^{18–20} This hierarchy has been employed to conceptualize the mechanism behind the thermodynamic and dynamic unusual behavior of water. This result suggests that the thermodynamic and the dynamic anomalies are not independent, but are related by the competition of two length scales: bonding and non bonding.²¹

Therefore it would be desirable that a model for water would be capable to capture not only the thermodynamic anomalies but also the dynamical anomalous behavior of water. In this paper we test if the TIP4P/ ϵ model also shows the dynamic anomalous region in the pressure versus temperature phase diagram observed in water. We compute the diffusion coefficient, D , versus temperature for various densities and temperatures. Then the location in the pressure versus temperature of the maximum and minimum of the diffusion coefficient D are compared with the density extrema and checked if the TIP4P/ ϵ has the hierarchy observed in the experiments. Our results are also compared with the TIP4P/2005^{12–14} model. Finally a summary of the thermodynamic, dynamic and structural properties of this model is compared with experiments and with the TIP4P/2005 mode in the spirit of the *grading* proposed by Vega et al.¹⁴

The remaining of this paper goes as follows. In the section 2 the force fields for the TIP4P/2005 and TIP4P/ ϵ are presented. In the section 3 the simulations are explained and in section 4 results are analysed. Conclusions are shown in section 5.

The Models

The different propositions for the four site models have in common the format illustrated in the Figure 1. The system is represented by the oxygen and the two hydrogens. The distance between the oxygen and the hydrogen is given by $r_{OH} = 0.9572$ while the angle between the

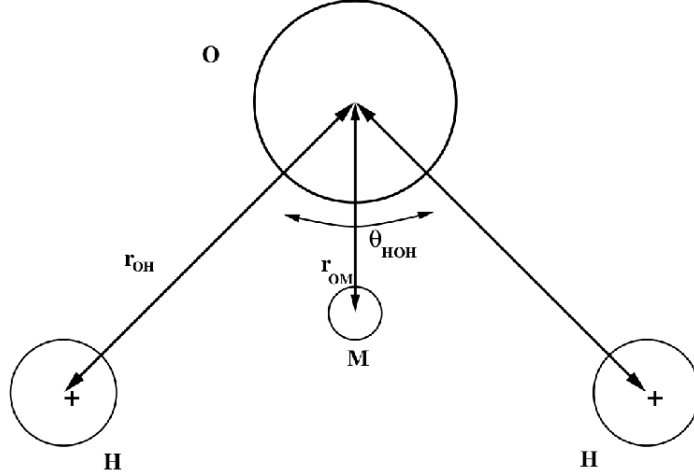


Figure 1: Model of four points for water: one oxygen, two hydrogens and a point M where the negative charge is located.

two hydrogens and the oxygen is $\theta_{HOH} = 104.52^\circ$. These quantities were set in order to give the appropriated ice form. The oxygen has mass $m_O = 15.999 \text{ g/mol}$ and the hydrogens have mass $m_O = 1.008 \text{ g/mol}$. The shared electrons between the hydrogens and the oxygen are closer to the oxygen. This is represented by the two positive charges, q_H , one at each hydrogen and a negative charge $q_M \approx 2q_H$ at a point M distant r_{OM} from the oxygen and located between the two hydrogens. Each water molecule i has a kinetic energy, K_i given by

$$K_i = \frac{1}{2} m_O v_i^2 \quad (1)$$

where v_i is the velocity of the molecule. Two water molecule interact through a potential with two contributions, a Lennard-Jones (LJ) between the oxygens and electrostatic interactions between the hydrogens and the negative charge at the point M, namely

$$u(r_{ij}) = 4\epsilon_{OO} \left[\left(\frac{\sigma_{OO}}{r_{ij}} \right)^{12} - \left(\frac{\sigma_{OO}}{r_{ij}} \right)^6 \right] + \frac{1}{4\pi\epsilon_0} \sum_{i=1}^3 \sum_{j=1}^3 \frac{q_i q_j}{r_{ij}} \quad (2)$$

where r_{ij} is the distance between atom i and j , q_i is the electric charge of atom i , ϵ_0 is the permittivity of vacuum, ϵ_{OO} is the LJ energy scale of the oxygen interactions and σ_{OO} the

diameter for an OO pair. The model has one LJ site and charge on the oxygen atom and additionally a charge on every hydrogen atom.

In this paper some thermodynamic, dynamic and structural properties of two force fields are compared: TIP4P/2005 and the TIP4P/ ϵ . For the first model the parameter, r_{OM} , ϵ_{OO} , q_H , ($q_M = 2q_H$) and σ_{OO} are selected by imposing that the model reproduces the maximum density at $T = 4^\circ C$ and atmospheric pressure. For the TIP4P/ ϵ the parameters are chosen so the model not only reproduces the density but also the dielectric constant at $T = 4^\circ C$ at atmospheric pressure. The parameters of these two force fields are given in the Table 1.

Table 1: Force field parameters for water models. The charge in site M is $q_M = -(2q_H)$.

Model	q_H/e	$q_M/e = 2q_H/e$	$r_{OM}/$	$\sigma_{OO}/\text{\AA}$	$(\epsilon_{OO}/k_B)/\text{K}$
TIP4P/ ϵ	0.9572	1.054	0.105	2.4345	93
TIP4P/2005	0.9572	1.1128	0.1546	2.305	93.2

Simulation details

All the simulations in this work have been done for a system of 500 molecules and employing molecular dynamic simulations in the NVT ensemble with the package GROMACS 4.5.²³ The equations of motion are solved using the leap-frog algorithm^{23,24} and the time step used was 2 fs. The Lennard-Jones potential has been switched from 10 up to a cut-off distance of 10 . Long range corrections were applied to the Lennard-Jones part of the potential (for both the energy and pressure).

Ewald summations were used to deal with electrostatic contributions. The real part of the Coulombic potential is truncated at 10 . The Fourier component of the Ewald sums was evaluated by using the particle mesh Ewald (PME) method²⁹ using a grid spacing of 1.2 and a fourth degree polynomial for the interpolation. The simulation box is cubic throughout the whole simulation and the geometry of the water molecules kept constant using the shake procedure.²⁷ Temperature has been set to the desired value with a Nosé Hoover thermostat.²⁵

The diffusion coefficient is calculated using the mean-square displacement averaged over different initial times, namely

$$\langle \Delta r(t)^2 \rangle = \langle [r(t_0 + t) - r(t_0)]^2 \rangle. \quad (3)$$

From Eq. (??), the diffusion coefficient may be obtained as follows:

$$D = \lim_{t \rightarrow \infty} \langle \Delta r(t)^2 \rangle / 6t. \quad (4)$$

The static dielectric constant is computed from the fluctuations²⁸ of the total dipole moment \mathbf{M} ,

$$\epsilon = 1 + \frac{4\pi}{3k_B T V} (\langle \mathbf{M}^2 \rangle - \langle \mathbf{M} \rangle^2) \quad (5)$$

where k_B is the Boltzmann constant and T the absolute temperature. The dielectric constant is obtained for long simulations at constant density and temperature or at constant temperature and pressure.

Results

First, the temperatures of maximum density for the different pressures were computed for both TIP4P/2005 and TIP4P/ ϵ models as follows. In the NVT ensemble this is done by relating the minimum of the isochores at the pressure versus temperature phase diagram. Using the Maxwell relation,

$$\begin{aligned} \left(\frac{\partial V}{\partial T}\right)_P &= -\left(\frac{\partial P}{\partial T}\right)_V \left(\frac{\partial V}{\partial P}\right)_T \\ \left(\frac{\partial \rho}{\partial T}\right)_P &= -\left(\frac{\partial P}{\partial T}\right)_V \left(\frac{\partial \rho}{\partial P}\right)_T \end{aligned} \quad (6)$$

the maximum of $\rho(T)$ versus temperature at constant pressure given by $(\partial \rho / \partial T)_P = 0$ is equivalent to the minimum of $(\partial P / \partial T)_\rho = 0$. While the former is suitable for NPT-constant

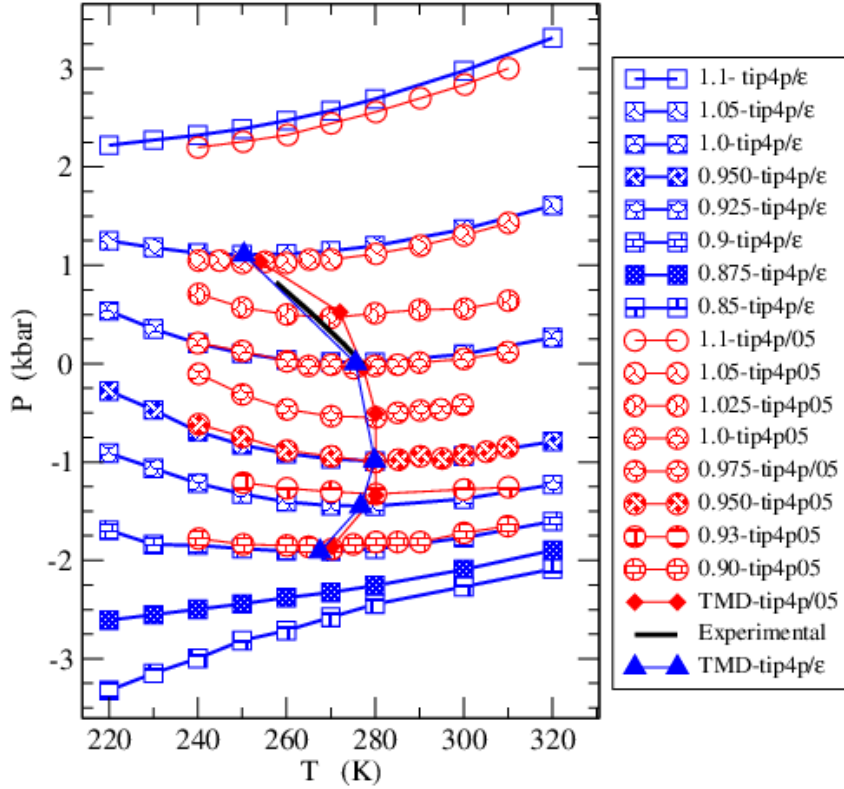


Figure 2: Pressure versus temperature phase diagram. The red circles are the isochores for the TIP4P/2005 model while the blue squares are the isochores for the TIP4P/ ϵ model. The minimum of the isochores show the TMD location for each model. The black line indicates the experimental results for the TMD. indicate isochores.¹⁶

experiments/simulations the latter is more convenient for our NVT-ensemble study, thus adopted in this work.

Figure 2 illustrates the pressure versus temperature phase diagram where the isochores for the TIP4P/2005 and for the TIP4P/ ϵ models are shown as red circles and blue squares respectively. The minimum of the isochores are also illustrated as red losanges for the TIP4P/2005 model and blue triangles for the TIP4P/ ϵ model. These lines locate the Temperature of Maximum Density (TMD). The simulations give a good agreement with the experimental results for the TMD represented by a black solid line. The two models are quite equivalent for the location of the TMD what is not surprising since both are adjusted to give the location of the density maximum at atmospheric pressure.

In addition to the thermodynamic anomaly the diffusion anomaly is also analyzed. Fig-

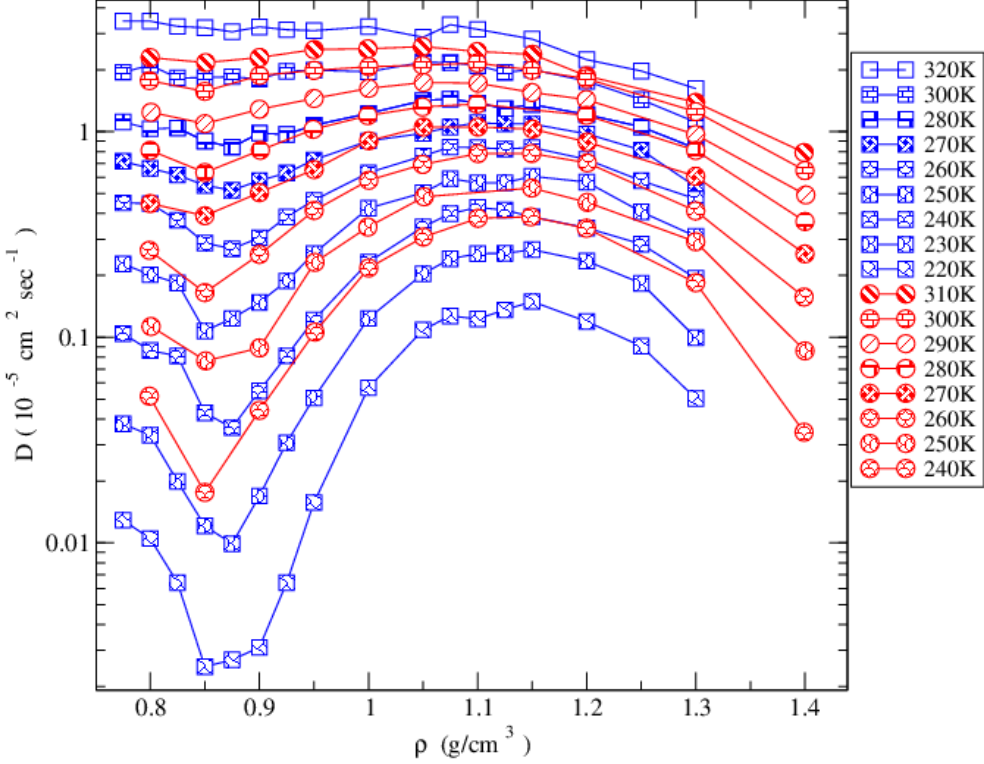


Figure 3: Diffusion coefficient versus density for various temperatures. The red circles illustrated D for the TIP4P/2005 model while the blue circles show the TMD for the TIP4P/ ϵ model. Both maximum of D .

ure 3 shows the diffusion coefficient versus density for both models for a range of temperatures. For both models de diffusion coefficient versus density graph has a maximum and minimum for various temperatures. The values of the temperature of the maximum and minimum diffusion coefficients are consistent with the values obtained by experiments.⁷ The pressures for the maximum and minimum D , however, give higher values when compared with the experimental results⁷ what might be attributed to the rigidity of both models.

The hierarchy of anomalies of the TIP4P/ ϵ model shown in the Figure ?? confirms the predicted behavior that the region in the pressure versus temperature phase diagram in which the diffusion anomaly is present involves the region where the density anomaly appears.¹⁸

We also check the behavior of the dielectric constant, ϵ , with the temperature and density. Figure 5 shows ϵ as a function of the temperature for different densities for the TIP4P/2005 (red circles) and TIP4P/ ϵ (blue squares) models. The TIP4P/2005 model shows much lower

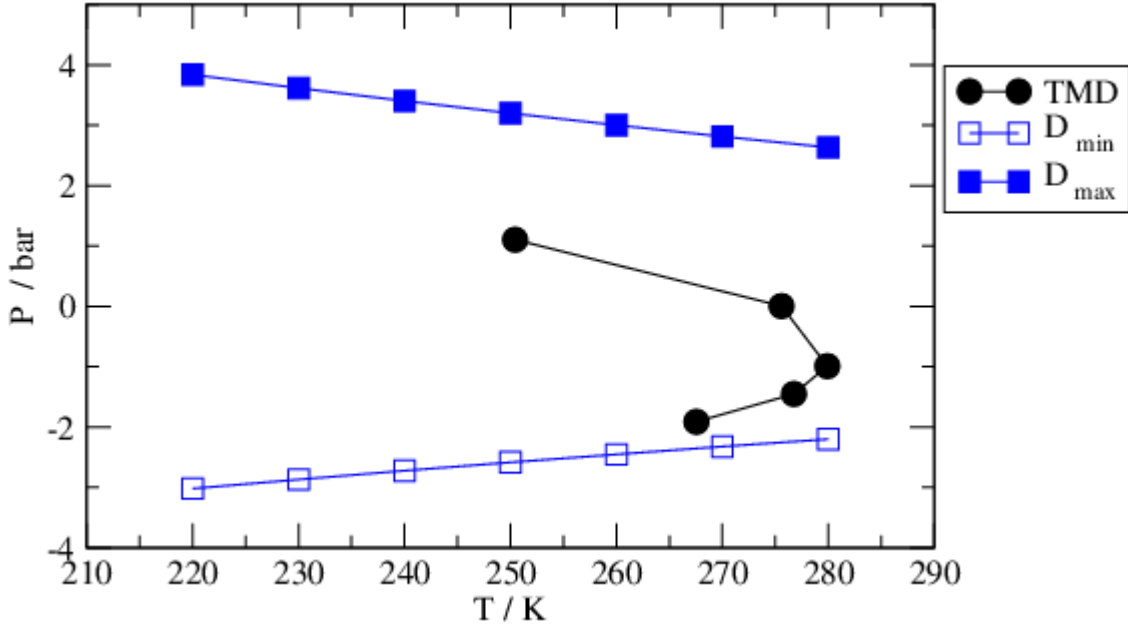


Figure 4: Pressure versus temperature phase diagram illustrating the temperature of maximum density (black filled circles) and the maximum (blue filled squares) and minimum (blue empty squares) of the diffusion coefficient for the TIP4P/ ϵ model.

values of dielectric constant when compared with the TIP4P/ ϵ model and experiments.¹⁷ The fact that the TIP4P/ ϵ gives a good estimate for the dielectric constant at room pressure and temperature is not surprising since the model was fitted to give this result. It is interesting to observe that for this result is also preserved for other values of temperatures.

Since the TIP4P/ ϵ does not provide a good evaluation of the pressure for the maximum of the diffusion anomaly it is important to verify if at high pressures the dielectric constant fails to agree with the experiments. Figure⁷ illustrates the dielectric constant versus pressure for different temperatures for the TIP4P/ ϵ model and experiments for $T = 300\text{ K}$. The agreement between simulations and experiments is good for the low pressures. Experimental data for higher pressures still need to be further explored.

In recent years Vega et al.¹⁴ proposed to evaluate the performance of water models by a measure. The models received a grade from zero to ten by checking how a finite group of properties from the liquid, solid and gas phases predicted by the model agree with experimental results. In addition to equilibrium thermodynamic properties, the measure includes

TIP4P/05 vs TIP4P/ ϵ

(Cte. ρ) ϵ vs T

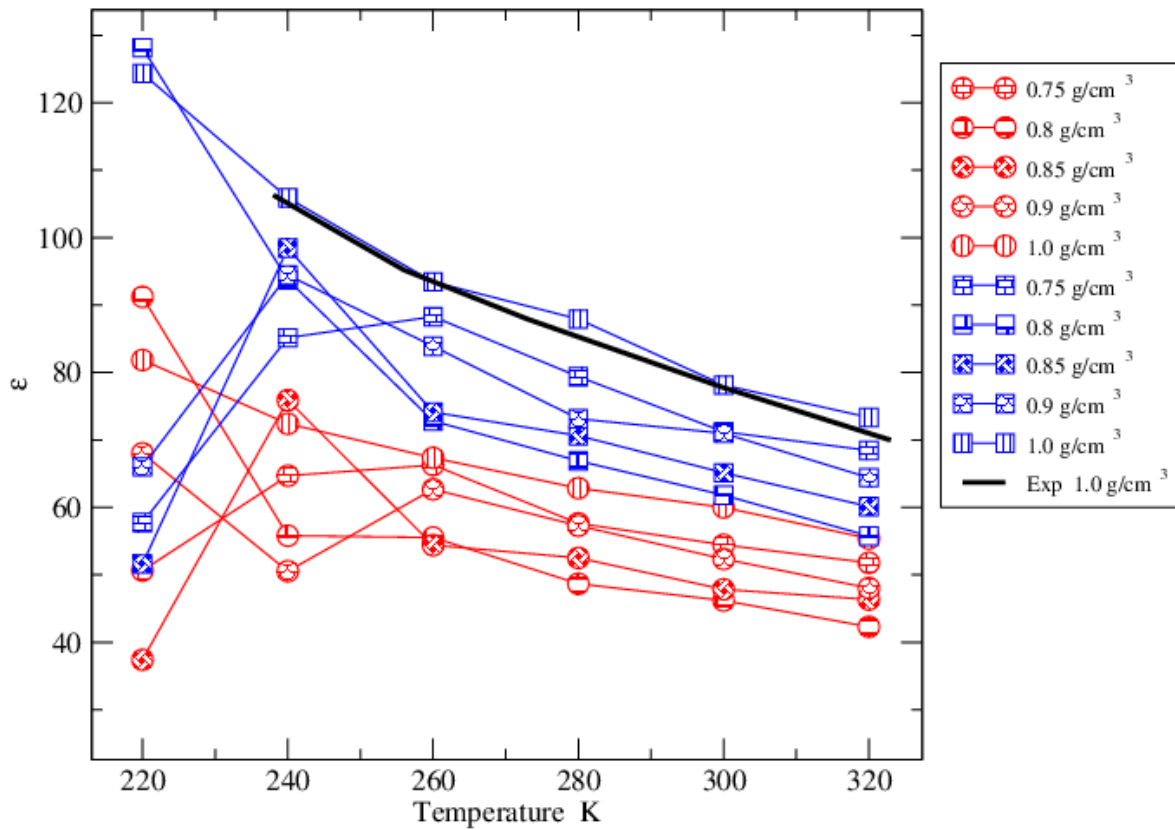


Figure 5: Dielectric constant versus temperature for different densities from $0.75\text{ g}/\text{cm}^3$ to $1\text{ g}/\text{cm}^3$ (from bottom to top) for the TIP4P/2005 (red circles) and for the TIP4P/ ϵ (blue squares) models. The experimental³¹ results (black solid line) are shown for $1\text{ g}/\text{cm}^3$.

dynamic properties and phase transition predictions. In order to answer to the logical criticism that the TIP4P/ ϵ model performs well in computing the dielectric constant but might fail in other properties in which TIP4P/2005 gives good agreements with experiments,³³ the measured proposed by Vega et al.¹⁴ was computed for the TIP4P/ ϵ model.

Table ?? shows the performance of the TIP4P/ ϵ model compared with the performance of the TIP4P/2005 for the properties proposed by Vega et al.¹⁴ Our results indicate that TIP4P/ ϵ gives good results not only for the dielectric constant, density and diffusion anomalies but also for the selected properties illustrated in the table.

COLOCAR AS REFERENCIAS NOS DADOS CALCULADOS POR OUTROS

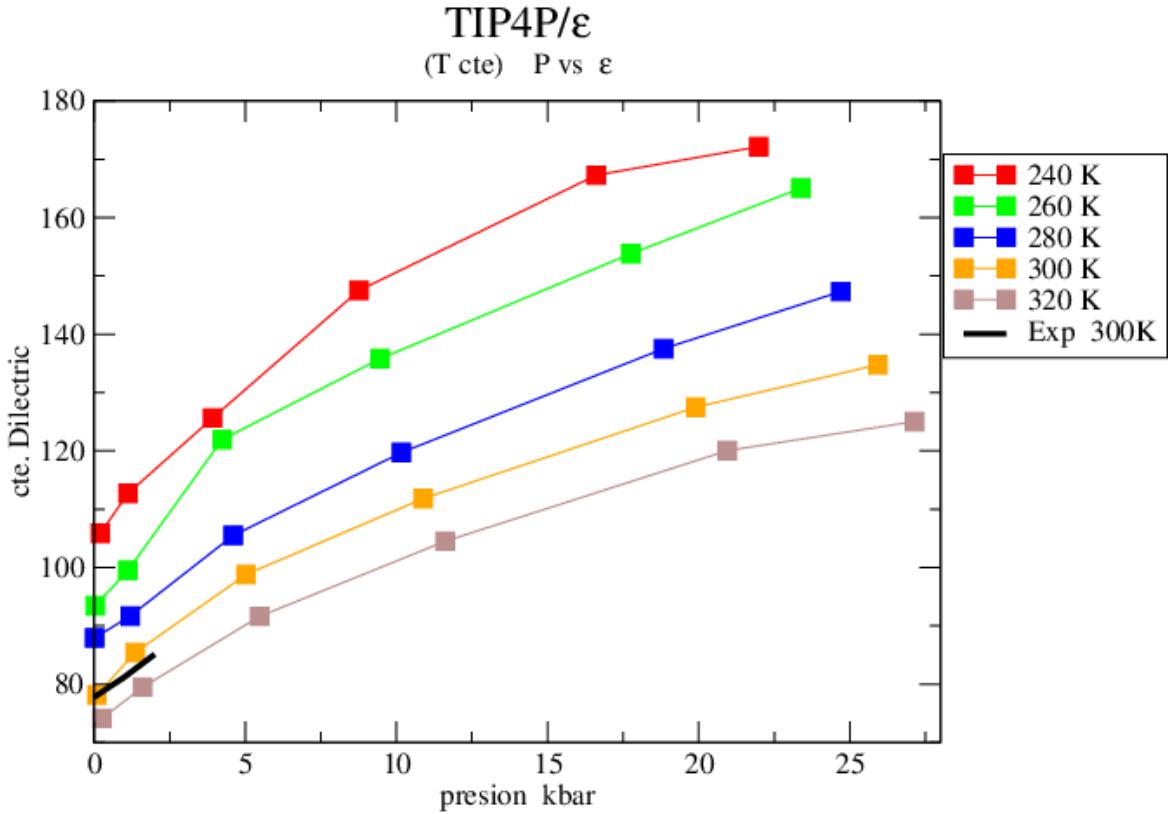


Figure 6: Dielectric constant versus pressure for $T = 240, 260, 280, 300, 320\text{ K}$ for the TIP4P/ ϵ model (circles) and for $T = 300\text{ K}$ for experiments³¹ (black squares).

POR QUE A NOTA DO TIP4P-2005 FOI 7.13 E NO PAPER DELES É 7.2?

Conclusions

In this paper we have computed explicitly the behavior of the density and diffusion anomalies for the TIP4P/ ϵ model showing that it gives similar results when compared with the TIP4P/2005 model.

Then, the behavior of the dielectric constant with the temperature and pressure was analyzed and compared with experimental results showing better agreement than the values obtained by other non-polarizable models.

Finally, the set of properties proposed by Vega et al. was computed. Our results that the performance of the TIP4P/ ϵ model is similar to the performance of the TIP4P/2005

Table 2

Property	Experiment data	Quantity TIP4P/05	Quantity TIP4P/ ϵ	% Tol.	Score TIP4P/05	Score TIP4P/ ϵ
Enthalpy of phase change / kcal mol ⁻¹						
ΔH_{melt}	1.44	1.16	1.24	5	6	7
ΔH_{vap}	10.52	11.99	11.74	2.5	4	5
Critical point properties						
T _c /K	647.1	640	675.45	2.5	10	8
ρ_c /g cm ⁻³	0.322	0.337	0.2993	2.5	8	7
p _c /bar	220.64	146	136	5	3	2
Surface tension/mN m ⁻¹						
γ_{300K}	71.73	69.3	69	2.5	9	8
γ_{450K}	42.88	41.8	43.8	2.5	9	9
Melting properties						
T _m /K	273.15	252	240	2.5	7	5
ρ_{liq} /g cm ⁻³	0.999	0.993	0.994	0.5	9	9
ρ_{sol} /g cm ⁻³	0.917	0.921	0.920	0.5	9	9
dp/dT (bar K ⁻¹)	-137	-135	-134	5	10	10
Orthobaric densities and temperature of maximum density TMD						
TMD/K	277	278	277	2.5	10	10
ρ_{298K} /g cm ⁻³	0.997	0.993	0.99628	0.5	9	10
ρ_{400K} /g cm ⁻³	0.9375	0.93	0.9368	0.5	8	10
ρ_{450K} /g cm ⁻³	0.8903	0.879	0.8842	0.5	7	9
Isothermal compressibility / 10 ⁻⁶ bar ⁻¹)						
κ_T [1 bar; 298 K]	45.3	46	45.8	5	10	10
κ_T [1 bar; 360 K]	47	50.9	49.1	5	8	9
Gas properties						
ρ_v [350 K] (bar)	0.417	0.13	0.026	5	0	0
ρ_v [450 K] (bar)	9.32	4.46	2.64	5	0	0
B2[450 K] (cm ³ mol ⁻¹)	-238	-476	-438	5	0	0
Heat capacity at constant pressure/cal mol ⁻¹ K ⁻¹						
C _p [liq 298 K; 1 bar]	18	21.1	19.1	5	7	9
C _p [ice 250 K; 1 bar]	8.3	14	11.9	5	0	1
Static dielectric constant						
ϵ [liq; 298 K]	78.5	58	78.3	5	5	10
ϵ [I _h ; 240 K]	107	53	63	5	0	2
Ratio	1.36	0.91	0.80	5	3	2
T _m -TMD-T _c ratios						
T _m [I _h]/T _c	0.422	0.394	0.355	5	9	7
TMD/T _c	0.428	0.434	0.410	5	10	9
TMD-T _m (K)	3.85	26	37	5	6	5
Densities of ice polymorphs/g cm ⁻³						
ρ [I _h 250 K; 1 bar]	0.92	0.921	0.919	0.5	10	10
ρ [II 123 K; 1 bar]	1.19	1.199	1.196	0.5	8	9
ρ [V 223 K; 5.3 kbar]	1.283	1.272	1.275	0.5	8	9
ρ [VI 225 K; 11 kbar]	1.373	1.38	1.377	0.5	9	9
EOS high pressure						
ρ [373 K; 10 kbar]	1.201	1.204	1.202	0.5	10	10
ρ [373 K; 20 kbar]	1.322	1.321	1.318	0.5	10	9
Self-diffusion coefficient/cm ² s ⁻¹						
ln D _{278K}	-11.24	-11.27	-11.3657	0.5	9	8
ln D _{298K}	-10.68	-10.79	-10.77	0.5	8	8
ln D _{318K}	-10.24	-10.39	-10.3	0.5	7	9
E _a kJ mol ⁻¹	18.4	16.2	16.3	5	8	8
Shear viscosity / mPa s						
η [1 bar; 298 K]	0.896	0.855	0.863	5	9	9
η [1 bar; 373 K]	0.284	0.289	0.307	5	10	8
Orientational relaxation time / ps						
τ_2^{HH} [1 bar; 298 K]	2.36	2.3	2.31	5	9	10
Structure						
$\chi^2(F(Q))$	0	8.5	8.5	5	8	8
χ^2 (overall)	0	14.8	14.8	5	7	7
Phase diagram						
Overall score (out of 10)					7.13	7.31

model¹⁴ with the exception of the dielectric constant for which the TIP4P/ ϵ shows a better agreement with the experimental results. We hope that this model might be suitable for studying mixtures and confined systems where the dielectric constant play an important role.

Acknowledgment

We thank the Brazilian agencies CNPq, INCT-FCx, and Capes for the financial support. We also thank the Centro Latino-Americano de Física (CLAF), Secretaría de Ciencia, Tecnología e Innovación del Distrito Federal de México (SECITIDF) and CONACYT (Project No. 232450) for financial support .

References

References

- (1) D. Eisenberg and W. Kauzmann, The Structure and Properties of Water (Oxford University Press, London, 1969).
- (2) M. Chaplin. Sixty Nine Anomalies of Water, <http://www.lsbu.ac.uk/water/anomlies.html>, accessed in May. 2015.
- (3) G. S. Kell, J. Chem. Eng. Data **20**, 97 (1975).
- (4) F. X. Prielmeier, F. X. and Lang, E. W. and Speedy, R. J. and Lüdemann, H.-D.Phys. Rev. Lett. **59**, 1128 (1987).
- (5) F. X. Prielmeier, E. W. Lang, E. W. and R. J. Speedy and H. -D. Ludemann, Ber. Bunsenges. Phys. Chem. **92**, 1111 (1988).

(6) L. Haar, J. S. Gallangher and G. S. Kell, NBS/NRC Steam Tables. Thermodynamic and Transport Properties and Computer Programs for Vapor and Liquid States of Water in SI Units, Hemisphere Publishing Co., Washington D. C., 1984.

(7) C. A. Angell, E. D. Finch, L. A. Woolf and P. Bach, *J. Chem. Phys.* **65**, 3063 (1976).

(8) P. H. Poole, F. Sciortino, U. Essmann and H. E. Stanley, *Nature* **360**, 324 (1992).

(9) J. D. Bernal and R. H. Fowler, *J. Chem. Phys.* **1**, 515 (1933).

(10) W. L. Jorgensen, J. Chandrasekhar and J. D. Madura, *J. Chem. Phys.* **79**, 926 (1983).

(11) G. Guillot, *J. Molec. Liq.* **101**, 219 (2002).

(12) J. L. F. Abascal and C. Vega, *J. of Chem. Phys.*, **123**, 234505 (2005).

(13) C. Vega, J. L. F. Abascal, M. M. Conde and J. L. Aragones, *Faraday. Discuss.* **141**, 251 (2009).

(14) C. Vega and J. L. F. Abascal, *Phys. Chem. Chem. Phys.* **13**, 19663 (2011).

(15) H. J. C. Berendsen, J. R. Grigera and T. P. Straatsma, *J. Phys. Chem.* **91**, 6269 (1987).

(16) R. A. Fine and F. J. J. Millero, *Chem. Phys.* **63**, 89 (1975).

(17) R. Fuentes-Azcatl and J. Alejandre, *J. Phys. Chem. B* **118**, 1263 (2014).

(18) J. R. Errington and P. D. Debenedetti, *Nature* **409**, 318 (2001).

(19) P. P. Netz, F. W. Starr, H. E. Stanley and M.C. Barbosa, *J. Chem. Phys.* **115**, 344 (2001).

(20) P. A. Netz, F. W. Starr, M. C. Barbosa and H. E. Stanley, *Physica A*, **314**, 470 (2002).

(21) A. B. de Oliveira, P. A. Netz, T. Colla and Marcia C. Barbosa *J. Chem. Phys.* **124**, 84505 (2006).

(22) M. Agarwal, M. Parvez and C. Chakravarty, *J. Phys. Chem. B* **115**, 6935 (2011).

(23) B. Hess, C. Kutzner, D. van der Spoel and E. Lindahl, *J. Chem. Theory Comput* **4**, 435 (2008).

(24) M. P. Allen and D. J. Tildesley, *Computer Simulation of Liquids*, Oxford University Press, Oxford, 1987.

(25) M. E. Tuckerman, Y. Liu, G. Ciccotti, G. J. Martyna, *J. Chem. Phys* **115**, 1678 (2001).

(26) Pedro Fernández Prini; International Association for the Properties of Water and Steam, 1997.

(27) J-P. Ryckaert, G. Ciccotti, H.J.C. Berendsen, *J. Comp. Phys.* **23**, 327 (1977).

(28) M. Neumann, *Molec. Phys.* **50**, 841 (1983).

(29) U. Essmann, L. Perera, M. L. Berkowitz, T. A. Darden, H. Lee and L. G. Pedersen, *J. Chem. Phys.* **103**, 8577 (1995).

(30) K. T. Gillen, D. C. Douglas and M. J. R. Hoch, *J. Chem. Phys.* **57**, 5117 (1972).

(31) P. Fernandez Prini; International Association for the Properties of Water and Steam; <http://www.iapws.org/relguide/IF97-Rev.pdf>, 2007 accessed in May. 2015.

(32) E. W. Lemmon, M. O. McLinden and D. G. Friend, *Thermophysical Properties of Fluid Systems*, NIST Chemistry WebBook, NIST Standard Reference Database , Eds. P.J. Linstrom and W.G. Mallard, <http://webbook.nist.gov>. USA, 2005.

(33) C. Vega, *Molecular Physics* , (2015).